

Regular Article

The effect of solvent polarity on wormlike micelles using dipropylene glycol (DPG) as a cosolvent in an anionic/zwitterionic mixed surfactant system

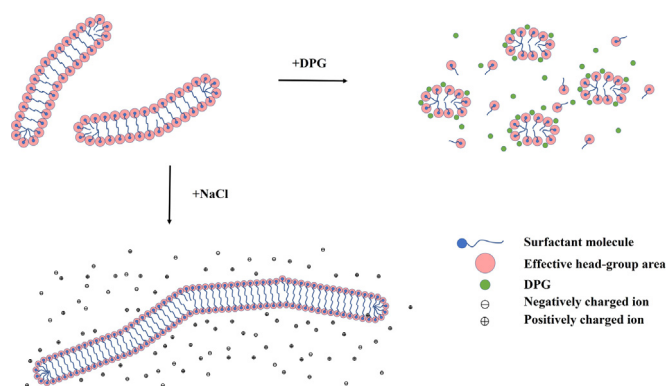


Hanqiu Jiang^a, Gregory Beaucage^{a,*}, Karsten Vogtt^a, Michael Weaver^b

^a Department of Chemical and Materials Engineering, University of Cincinnati, Cincinnati, OH 45221-0012, United States

^b P&G Analytical Sciences, 8700 Mason-Montgomery Rd, Mason, OH 45040, United States

GRAPHICAL ABSTRACT



ARTICLE INFO

Article history:

Received 16 July 2017

Revised 27 August 2017

Accepted 28 August 2017

Available online 31 August 2017

Keywords:

Small angle neutron scattering

Worm-like micelle

Ellipsoid

Dipropylene glycol

Cosolvent

Dielectric constant

ABSTRACT

Hypothesis: The behavior/properties of micellar solutions are governed by Coulombic interactions that are influenced by the polarity of the surfactant head groups, hydrophobic tails, and solvent molecules. The addition of co-solvent should have a direct impact on solvent polarity and the size of the micelles are expected to decrease accordingly.

Experiments: In this study, a mixed surfactant system is studied composed of a common anionic surfactant, sodium laureth sulfate-1, modified by a zwitterionic surfactant, cocamidopropyl betaine in deuterated water. In this system, worm-like micelles (WLMs) are formed. The influence of a co-solvent, dipropylene glycol (DPG) in the present of high salt content, is investigated. DPG primarily modifies the dielectric constant of the solvent.

Findings: It was found that the addition of DPG slightly decreased the micelle radius, but dramatically reduced the persistence length as well as the contour length of the micelles. The relative dependence of contour length on salt concentration is not significantly changed. Thus, it is shown that the self-assembled structure can be tuned by adjusting solvent polarity without affecting the relative tunability of the WLM/ellipsoidal structure through counter ion concentration.

© 2017 Elsevier Inc. All rights reserved.

* Corresponding author.

E-mail address: gbeaucage@gmail.com (G. Beaucage).

1. Introduction

Amphiphilic molecules in aqueous solutions can self-assemble into elongated, semi-flexible aggregates, also known as worm-like micelles (WLMs) [1]. The ability to reversibly self-assemble gives unique properties to WLMs and has led to widespread application [2]. As the behavior/performance of the WLM products depend largely on the self-assembled nanostructure, it is important to control the dynamic equilibrium between the self-assembled state and dispersed surfactant molecules. The main idea of manipulating the equilibrium is to control the balance between solvent incompatibility with the tail groups, which drives the formation of micelles, and solvent electrostatic interactions with the head groups which favor the dispersion of surfactant molecules [3]. Co-solvents/co-surfactants have long been employed to alter the dynamic balance of micellar systems [7] and the performance of surfactants, such as in pharmaceutical formulation [4] and oil recovery [5,6]. For example, in oil recovery [5,6], formulas modified by co-solvents show increased oil recovery with reduced viscosity and surface tension. Economically efficient and environmental friendly features are also reasons that co-solvents/co-surfactants are extensively used.

Non-aqueous polar molecules, glycols or alcohols, are of particular interest as co-solvents/co-surfactants due to their relatively high dielectric constant, cohesive energy density and their ability to form hydrogen bonds with water molecules [8]. The term co-solvent or co-surfactant is chosen depending on the solubility of the alcohol in water and their consequent partitioning into the micelle or solvent phase. Usually, short chain alcohols with higher polarity tend to stay in the water phase [10]. The decrease of micelle size upon addition of this kind of alcohol is explained by the change of solvent properties. Thus, short chain alcohols are usually considered as co-solvents. Alcohol molecules with longer alkyl chains tend to show weaker polarity [9] that leads to poor miscibility of long chain alcohols in water and their increasing partition into the micellar phase. Long chain alcohols are often considered co-surfactants.

In order to understand the impact of co-solvents on micellar systems, two main aspects have been studied, the critical micelle concentration (CMC) and the size of the micelles. Different combinations of nonionic surfactant, ionic surfactant, and mixed surfactant have been studied [8,10–19]. As a key parameter of micellization, the CMC is defined as the concentration above which micelles form. Further added surfactant goes directly into the micellar phase while the concentration of surfactant monomers remaining dispersed in the solution is more or less constant at the CMC [20] in a dynamic equilibrium between micelles and free surfactant monomers [21]. Upon addition of a non-aqueous, polar co-solvent, the reduced hydrophobic interaction between the surfactant tails and solvent molecules leads to an increase in the solubility of free surfactant monomers relative to micelles thus shifting the CMC to a higher value. Such an increase in the CMC has been extensively observed [8,10–17]. In addition to an increase in the CMC, a decrease of the micellar size was reported in these studies. This increase in size was associated with increased surface curvature due to larger incompatibility between the head groups and solvent, and a concomitant increase in repulsion between the charged head groups [8,10–17]. However, this is not a universal observation and the explanation does not apply to all systems. Others report a reverse trend that the size of micelles increase with the addition of co-solvents. Penfold, Alexandridis et al. [18,19] reported an increase in micelle size and a lower concentration onset of CMC of surfactant systems with increasing co-solvent concentration using small angle neutron scattering (SANS). This contrary trend was explained by the dehydration of the surfactant

head groups due to the relatively low polarity of the co-solvent molecules, which caused a reduction of the effective head group area and led to an increase in the micelle diameter due to a lower surface curvature. No clear boundary was drawn between the two tendencies. The actual impact of a certain type of co-solvent on a specific micelle system still remains elusive, which makes the study of individual cases necessary. Furthermore, although numerous experiments have been conducted on this topic, most of the research was confined to spherical micelles. A fundamental understanding of the effect of co-solvents on WLMs is still very limited.

In this work, it was chosen to study the diol dipropylene glycol (DPG) as a co-solvent in a mixed surfactant system with high salt content. DPG is a commonly used stability modifier for detergents due to its low toxicity and relatively high dielectric constant. The addition of glycol to the aqueous phase leads to a decrease in the dielectric constant, and the cohesive energy density, as well as breakup of the water structure [22]. The decrease of the dielectric constant enhances the long-range electrostatic interactions between charged head groups and solvent disproportionately. In this paper, solvent dielectric characteristics are considered as a key factor that could alter the micellization process. Neutron scattering is used to quantify structural changes associated with changes in solvent polarity.

Upon addition of counterions, screening of electrostatic repulsions between headgroups leads to a decrease in effective head-group area. At high counterion concentrations, spherical micelles transition through ellipsoidal, rod-like, and worm-like structures that display a diameter, persistence length, and contour length rather than the single size associated with a spherical micelle. The transition between spherical and ellipsoidal micelles in surfactant concentration is sometimes called a second CMC [23]. Adjustment of salt concentration is often used to control the contour length and viscoelastic properties of WLMs [24]. Previous studies in water-alcohol systems have been limited to studies of micellization of spherical micelles in terms of the CMC. The impact on WLM structures with high counter ion concentrations and the impact of solvent polarity on counter ion control of WLM structure are absent from the literature.

In this paper, we investigate the change of WLM/ellipsoidal structure due to a change in solvent polarity using SANS. DPG was selected as a co-solvent due to its extensive use in industrial formulations of cosmetic products. The aim of this work is to understand the effect of solvent polarity on the structure of WLMs at high salt content and to observe its effect on control over WLM contour length and viscoelastic properties through variation in salt concentration with mixed surfactants.

2. SANS model for WLM structure

Above the CMC, formation of spherical micelles occurs. A secondary CMC is observed at the onset of anisotropic cylindrical and ellipsoidal micelles that accommodate reduced head group repulsion as counter ion screening increases with increased salt concentration. Once an asymmetric structure forms the structure is largely governed by the end cap energy relative to the energy of the cylindrical structure. High end-cap energy encourages growth of very long micelles that can be thread-like with contour lengths on the order of microns. There is a wide distribution of lengths in such a thread-like micelle population that is proposed to follow an exponential number distribution [25] similar to synthetic polymers grown from step-growth polymerization.

Worm-like chains have been characterized using a persistent chain model or using a Kuhn chain model. The persistent chain model relies on a statistical description of the persistence length

while the Kuhn model utilizes discrete rod-like segments that are analogous to the persistence units. The Kuhn model is the basis for most rheological predictions for WLM systems. For this study, we model the chains using a Kuhn model based on radially polydispersed cylindrical subunits of length L_1 which is often termed the “persistence length”, l_p , of the worm-like chain but actually reflects the Kuhn length. (For Gaussian chains of infinite length $L_1 \sim 2l_p$.) The radius, R_1 , is modeled with a log-normal size distribution using the dimensionless geometric standard deviation of this distribution as a free fitting parameter, σ_g . “z” of these Kuhn segments are gathered into chains following a self-avoiding walk of dimension $5/3$. The model allows for branching of these self-avoiding chains which leads to a fractal dimension, d_f , larger than $5/3$. The contour length for the chain is given by $L_2 = zL_1$, where L_2 includes branches and the minimum conductive path with a minimum dimension of $d_{\min} = 5/3$ [26]. L_2 is calculated rather than directly measured and reflects the extended length of a WLM. The actual size is much smaller since the chain is convoluted and possibly branched. A fitting function for scattering that follows this model has been published previously [27],

$$I(q) = I_1(q) + I_2(q) \quad (1)$$

where

$$I_1(q) = \int_0^\infty N(R_1)G_1P_{\text{cyl}}(q, R_1, L_1)dR_1 \\ = \phi_{MS}\langle\Delta\rho\rangle^2 \frac{\int_0^\infty R_1^2 N(R_1)V_{\text{cyl}}P_{\text{cyl}}(q, R_1, L_1)dR_1}{\int_0^\infty R_1^2 N(R_1)dR_1} \quad (2)$$

and

$$I_2(q) = G_2e^{-q^2R_{g,2}^2/3} + B_2e^{-q^2R_{g,1}^2/3}(q^*)^{-d_f,z} \quad (3)$$

where

$$q^* = \frac{q}{\left[\text{erf}\left(\frac{1.06qR_{g,2}}{\sqrt{6}}\right)\right]^3} \quad (4)$$

In Eq. (2), $N(R_1)$ is a log-normal distribution function for cylindrical radii, G_1 is the Guinier prefactor for level 1, and $P_{\text{cyl}}()$ is the cylindrical form factor. V_{cyl} is the volume of the cylindrical subunit. $\phi_{MS}\langle\Delta\rho\rangle^2$ is the inherent contrast for the WLM, ϕ_{MS} is the volume fraction of mixed surfactant and $\Delta\rho$ is scattering length density difference, as discussed below. In Eq. (3), G_2 is the Guinier prefactor for level 2, $R_{g,i}$ is the radius of gyration for level “i”, and B_2 is the power-law prefactor for level 2. These parameters, and the scattering function are fully described in [27]. Particularly, $z = G_2/G_1 + 1$, and $R_{g,1}^2 \approx L_1^2/12 + R_1^2/2$.

3. Materials and methods

The surfactant mixtures were made from a common anionic surfactant, sodium laureth-1 sulfate (SLE1S, commercially available as STEOLCS-170) at 0.179 wt% (5.70 mM), and a zwitterionic surfactant, cocamidopropyl betaine (CAPB, commercially available as Amphosol HCA-HP) at 0.021 wt% (0.648 mM) in deuterated water. (Both surfactants are available from Stepan Chemical, Northfield, Ill.) Deuterated water is employed to enhance the scattering contrast in SANS measurements. This binary surfactant mixture was chosen since it has been seen to produce stable WLM structures and because it serves as a model for more complicated commercial surfactant mixtures. The influence of the co-solvent DPG (3.72 wt%, 0.277 M) was studied. DPG (Sigma-Aldrich, St Louis, MO) was used as received. The composition was found to be a mixture of isomers containing approximately 33.4% 1,1-oxybis-2-propanol; 24.1% 2,2-oxybis-1-propanol; 7.9% 3,3-oxybis-1-propanol and 34.6% 2-(2-hydroxypropoxy)-1-propanol

using GCMS (HP6980 GC with 5973 MSD/FID detection; Agilent Technologies). A series of salt concentrations, NaCl at 3.01, 3.56, 4.01, 4.50, 5.00 wt% (0.515 M, 0.609 M, 0.686 M, 0.770 M, 0.856 M) with and without DPG was investigated at 25 °C in order to understand the effect of DPG on the structure of WLMs in the context of variable counter ion concentration.

The NaCl concentration in the CAPB paste was measured using an auto-titration procedure following the AOCS (American Oil Chemists' Society) official method Db 7b-55 [28]. The NaCl contained in the original CAPB paste was counted towards the overall salt concentration.

SANS data for samples with no DPG were measured on the GP-SANS instrument at Oak Ridge National Laboratory, Oak Ridge, Tennessee, USA. SANS data for samples with DPG were measured on the NG7 SANS instrument at the National Institute of Standards and Technology, Gaithersburg, Maryland, USA. Data were reduced by procedures provided by the beam lines [29]. Data sets after reduction and background correction were fitted using the fitting function proposed by Vogtt [27].

Flow viscosity measurements were made on the surfactant solutions using a TA Instruments DHR3 rheometer equipped with DIN concentric cylinders geometry (cup diameter = 30.38 mm, cylinder outer diameter 27.97 mm) at 25 °C. The Couette geometry utilizes Peltier temperature control. A solvent trap was used to maintain environmental integrity. The flow curves were collected using Trios software. After the sample reached temperature, a 300 s equilibrate time ensued before commencing the flow experiment. Because the viscosity of these solutions was low, but possibly shear thinning, individual steady state flow curves were collected at 10, 5, 2, 1, 0.5, 0.2, 0.1, and 0.05 s⁻¹ shear rates using the Trios software steady state sensing with 60 s sample period and 3% tolerance at each shear rate. This procedure allowed the zero-shear viscosity plateau to be verified and the onset of shear thinning, if it occurred, to be documented. The viscosity of the DPG-NaCl/D₂O solutions were measured using an Anton Paar Lovis ME2000 rolling ball viscometer with a 1.59 mm capillary. The solvent viscosity was measured at 25 °C after it was equilibrated. The specific viscosity was calculated as $\eta_{sp} = (\eta_0/\eta_s) - 1$ using the viscosity observed from the zero-shear viscosity plateau η_0 from the surfactant samples and the solvent viscosity η_s data from the Lovis viscometer.

4. Results and discussion

Fig. 1 shows the change in scattered intensity with the addition of DPG. A log-log plot of scattered intensity versus scattering vector is shown. At intermediate q , 0.015 to 0.03 Å⁻¹, the data displays a regime of -1 power-law scaling for 1-dimensional Kuhn units. At lower q 0.001 to 0.006 Å⁻¹ deviation from this -1 power-law indicates the presence of a structure with higher mass fractal dimension with a power-law slope close to $-5/3$ for a self-avoiding walk. This is the convoluted path of the WLM structure. A dramatic reduction in the WLM contour length is evident on addition of DPG. At the high- q limit of the -1 power law a Guinier regime (exponential decay) is reflected in a knee feature, 0.04 to 0.1 Å⁻¹. The higher q cutoff of this knee from the steep decay at high- q (Porod's Law with -4 slope) indicates a higher- q or smaller size for the cylindrical radius in the presence of DPG. Features at the highest- q , >0.2 Å⁻¹, are dominated by background but could reflect local structure of the micelle surface layer. The fit parameters which were defined in the SANS model section are listed in Tables 1 and 2. The large-scale structural features (L_2 and z) for the samples with no DPG at higher salt concentration have relatively large error bars because the size scale of the micelles is approaching the low- q limit of the SANS measurement.

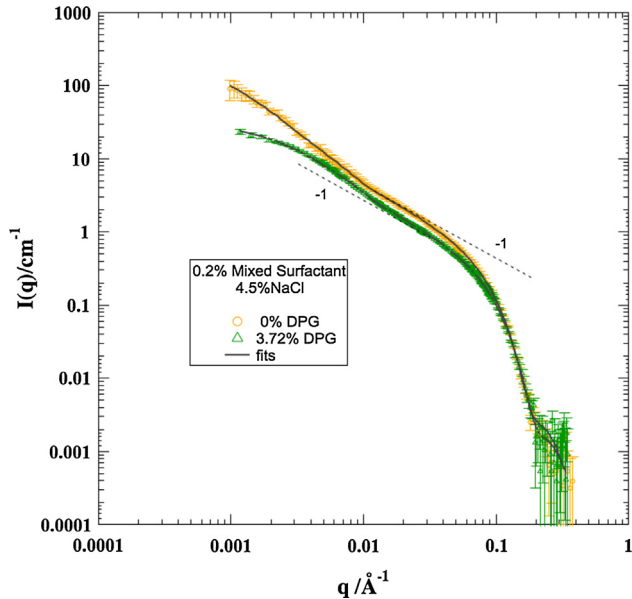


Fig. 1. Log-log plot of scattered intensity, $I(q)$, versus scattering vector, q . Low- q corresponds to large sizes and the difference in intensity in this region reflects a reduction in contour length for the DPG samples, $0.001\text{--}0.006\text{ \AA}^{-1}$. Between 0.04 and 0.1 \AA^{-1} , the difference between the curves reflects a slightly smaller WLM radius in the presence of DPG. The region indicated by the -1 power-law slope reflects the cylindrical Kuhn structure. Deviation from this -1 power-law at low- q indicates the presence of a convoluted WLM structure. (Complete data and fits from this study are given in the [supplemental material](#).)

4.1. Determination of DPG location

Tables 1 and 2 list the measured contrast, $\phi\Delta\rho^2$, for the WLMs with and without DPG. SANS for this system is not sensitive to the head group layer of the WLMs since the dense hydrogen-rich micellar core, with a negative scattering length density (SLD) of $\sim -0.3 \times 10^{10}\text{ cm}^{-2}$, is the main contributor to the measured scattering contrast [27]. D_2O and DPG have a SLD of $\sim 6.4 \times 10^{10}\text{ cm}^{-2}$ and $\sim 0.23 \times 10^{10}\text{ cm}^{-2}$ respectively. Theoretically the scattering contrast between the solvent phase and micelles can be calculated according to the following equation,

$$\langle\Delta\rho\rangle^2 = \left[\left(\frac{\phi_{\text{D}_2\text{O}}\rho_{\text{D}_2\text{O}} + \phi_{\text{DPG1}}\rho_{\text{DPG}}}{\phi_{\text{DPG1}} + \phi_{\text{D}_2\text{O}}} \right) - \left(\frac{\phi_{\text{MS}}\rho_{\text{MS}} + \phi_{\text{DPG2}}\rho_{\text{DPG}}}{\phi_{\text{DPG2}} + \phi_{\text{MS}}} \right) \right]^2 \quad (5)$$

where ρ and ϕ are the scattering length density and volume fraction of different compounds in the system respectively. $\phi_{\text{MS}} \approx 0.002$ stands for the volume fraction of mixed surfactant. ϕ_{DPG1} and

ϕ_{DPG2} are the volume fraction of DPG in the solvent phase and in the micelles respectively. If DPG dissolved totally in D_2O only a small decrease of the solvent phase SLD would occur since DPG is at a low concentration and has a scattering length density much smaller than that of D_2O , while the partitioning of DPG to the core of the micelles would lead to a larger decrease in the measured scattering contrast, as both the amount and scattering length density of surfactants are much smaller than those of D_2O . Fig. 2 depicts the change in the calculated $\phi_{\text{MS}}\langle\Delta\rho\rangle^2$ with increasing percentage of DPG in the micellar phase. The term $\phi_{\text{MS}}\langle\Delta\rho\rangle^2$ arises from Eq. (2) where it reflects the fitted contrast for the WLM. The results indicate that no perceptible partitioning of DPG occurs to the core of the micelles. The minor difference in the measured and calculated values might be attributed to surfactant concentration differences from normal accuracy during sample preparation as well as the measurement error. These results are sufficient to conclude that DPG works as a co-solvent in this system and is primarily in solution.

4.2. Impact of DPG on micelle structure

Fig. 3(a) indicates a statistically relevant slight decrease ($\sim 8\%$) in WLM/rod radius in the presence of DPG that is not strongly affected by salt concentration. Fig. 3(b) shows the geometric standard deviation for the log-normal distribution of micelle radii of the samples. For samples without DPG a relatively constant standard deviation was obtained around 0.18. For samples with DPG, the standard deviation of the cross-sectional radius increased with salt concentration and reaches the same value as that of no DPG samples at 4% and higher salt concentration. In Table 2 the number of cylindrical subunits, z , of DPG samples at low salt concentrations are reported as 1 and 3.1. This suggests the presence of rod-like micelles instead of typical WLMs. At 3.01% NaCl in the presence of DPG the fit is to a cylindrical rod, $z = 1$, rather than a convoluted chain, $z > 1$. This may influence the low value of the geometric standard deviation seen in Fig. 3b when comparing with a convoluted worm-like chain model. The relatively lower σ_g observed at low salt concentration in the presence of DPG may reflect differences in the fit function when $z = 1$ rather than sample characteristics. The results suggest that the presence of DPG may not alter the breadth of the size distribution of the cylindrical radius at various salt concentrations.

Fig. 4 shows the dependence of WLM Kuhn length on salt concentration and addition of DPG. For the first point in the presence of DPG at 3% NaCl the sample has only one Kuhn rod unit in the structure, $z = 1$. For that point, the comparison with the chain in the absence of DPG, $z = 9$ in Table 1, is complicated since a WLM and rod-like structure are being compared. Other than the 3% NaCl points, the Kuhn length is consistently about 15% shorter in the presence of DPG. Chain persistence reflects the rigidity of the chain.

Table 1

Micellar size parameters obtained through fitting for 0.2 wt% of mixed surfactant (MS) under various salt conditions in D_2O . Values with errors were fit.^a

0.2% MS No DPG	3.01% NaCl	3.56% NaCl	4.01% NaCl	4.5% NaCl	5.0% NaCl
$\phi_{\text{MS}}\langle\Delta\rho\rangle^2 10^{19}\text{ cm}^{-4}$	0.764 ± 0.003	0.889 ± 0.003	0.846 ± 0.003	1.029 ± 0.003	0.893 ± 0.003
$R_1/\text{\AA}$	18.9 ± 0.1	19.5 ± 0.1	19.2 ± 0.1	19.2 ± 0.1	19.3 ± 0.1
$\sigma_{R,1}$	0.183 ± 0.006	0.166 ± 0.005	0.185 ± 0.005	0.190 ± 0.004	0.194 ± 0.005
$L_1/\text{\AA}$	540 ± 30	630 ± 30	660 ± 40	660 ± 40	610 ± 20
G_2/cm^{-1}	41 ± 6	90 ± 20	120 ± 20	200 ± 100	300 ± 100
$R_{g,2}/\text{\AA}$	1400 ± 200	2000 ± 200	1900 ± 600	1700 ± 800	2000 ± 600
z	9 ± 1	14 ± 2	18 ± 3	20 ± 10	50 ± 20
$d_{f,2}$	1.67	1.67	1.8 ± 0.2	2.0 ± 0.2	2.1 ± 0.1
$L_2/\text{\AA}$	4900 ± 800	9000 ± 2000	$12,000 \pm 2000$	$13,000 \pm 7000$	$30,000 \pm 10,000$

^a $\phi_{\text{MS}}\langle\Delta\rho\rangle^2$ is the volume fraction of mixed surfactant multiplied with the scattering contrast. R_1 is the cross-sectional radius of the cylindrical subunits. $\sigma_{R,1}$ is the dimensionless geometric standard deviation of R_1 . L_1 is the length of the cylindrical subunits. G_2 is the prefactor of Guinier law. $R_{g,2}$ is the radius of gyration of large scale structure. z is the number of cylindrical subunits contained in a micelle. $d_{f,2}$ is the fractal dimension of large scale structure. L_2 is the average contour length of the micelles.

Table 2Micellar size parameters obtained through fitting for 0.2 wt% of mixed surfactant (MS) under various salt conditions in 3.72 wt% DPG and D₂O. Values with errors were fit.^a

0.2%MS 3.72%DPG	3.01% NaCl	3.56% NaCl	4.01% NaCl	4.5% NaCl
$\phi_{MS}(\Delta\rho)^2 \cdot 10^{19} \text{ cm}^{-4}$	0.830 ± 0.004	0.847 ± 0.004	0.810 ± 0.005	0.835 ± 0.005
$R_1/\text{\AA}$	18.2 ± 0.1	18.1 ± 0.2	17.6 ± 0.2	18.1 ± 0.2
$\sigma_{R,1}$	0.13 ± 0.01	0.15 ± 0.01	0.19 ± 0.01	0.18 ± 0.01
$L_1/\text{\AA}$	570 ± 6	545 ± 7	539 ± 5	582 ± 5
G_2/cm^{-1}	N/A	10 ± 1	14.2 ± 0.8	27 ± 1
$R_{g,2}/\text{\AA}$	N/A	1070 ± 60	950 ± 30	1170 ± 40
z	1	3.1 ± 0.2	4.1 ± 0.04	5.1 ± 0.04
$d_{f,2}$	1	1.67	1.67	1.67
$L_2/\text{\AA}$	570 ± 6	1700 ± 100	2200 ± 100	3600 ± 100

^a $\phi_{MS}(\Delta\rho)^2$ is the volume fraction of mixed surfactant multiplied with the scattering contrast. R_1 is the cross-sectional radius of the cylindrical subunits. $\sigma_{R,1}$ is the dimensionless geometric standard deviation of R_1 . L_1 is the length of the cylindrical subunits. G_2 is the prefactor of Guinier law. $R_{g,2}$ is the radius of gyration of large scale structure. z is the number of cylindrical subunits contained in a micelle. $d_{f,2}$ is the fractal dimension of large scale structure. L_2 is the average contour length of the micelles.

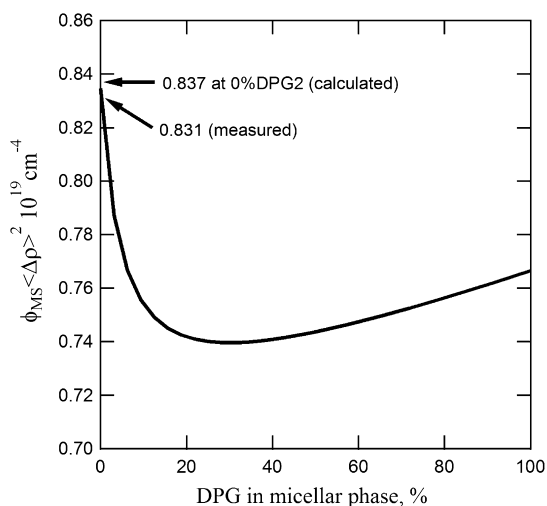


Fig. 2. Calculated scattering contrast ($\phi_{MS}(\Delta\rho)^2$) versus percentage of DPG participating in the micellar phase. Solid line is calculated from Eq. (5).

The thinner WLMs associated with the presence of DPG, Fig. 3(a), are therefore more flexible.

The impact of solvent polarity on micellization of surfactants has been explained through various mechanisms [13,14,30,31]. It is generally accepted that the change of the properties of the surrounding aqueous solution is the main cause of the reduction of

micelle size with co-solvent addition for ionic surfactant systems [31]. DPG has a considerably lower dielectric constant ($\epsilon_r = 19.8$), than that of D₂O ($\epsilon_r = 77.9$) [32]. The dielectric constant reflects the solvent's ability to screen charged species from each other via polarization of the solvent molecules. Consequently, mixtures of DPG and D₂O, with lower dielectric constants, promote electrostatic interactions between surfactant head groups. The increased repulsion among the ionic head groups may lead to an increase of the micellar surface curvature, resulting in the formation of smaller aggregates. That is, the radius and persistence length of cylindrical subunits (R_1 and L_1) are expected to become smaller with the addition of DPG. The increased head group interaction stabilizes chain ends relative to cylindrical segments leading to a reduction in the contour length, L_2 , since the end groups have greater curvature. Consistent with the literature and simulation result [33], R_1 , L_1 and L_2 of micelles in 3.72 wt% DPG are smaller than those in pure D₂O as depicted in Figs. 3(a), 4 and 5.

4.3. Comparison of thermodynamic impacts of DPG and salt

Fig. 5 shows that the average contour length of WLMs increases exponentially with salt concentration, $L_2 = L_{2,0} \exp(k\phi_{NaCl, wt})$. While the exponential growth constant is identical for samples with and without DPG ($k = 90$), the prefactor, $L_{2,0}$, differs considerably (60 Å versus 330 Å). The increase of micelle length with salt concentration can be explained by greater electrostatic screening with increasing salt concentration which reduces the effective head group area and favors the cylindrical over end-cap surfactant packing.

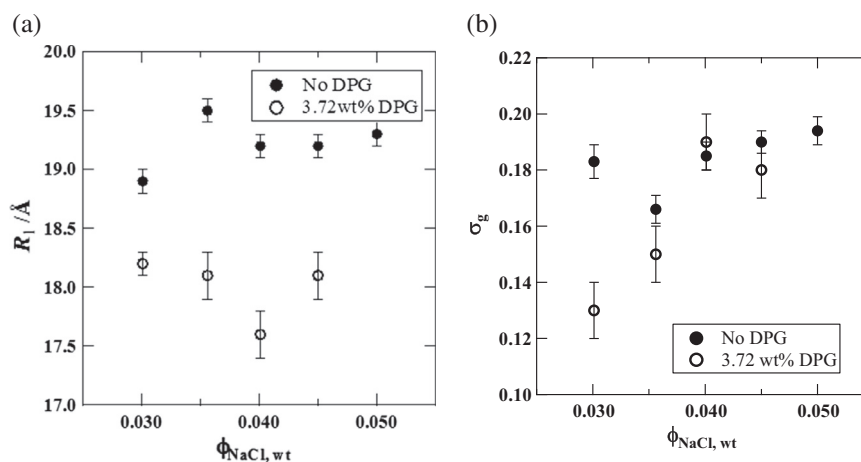


Fig. 3. (a) WLM/ellipsoid radius, R_1 , as a function of weight fraction salt (b) Dimensionless geometric standard deviation, σ_g , of the log-normal distribution for the cylindrical radius as a function of weight fraction salt.

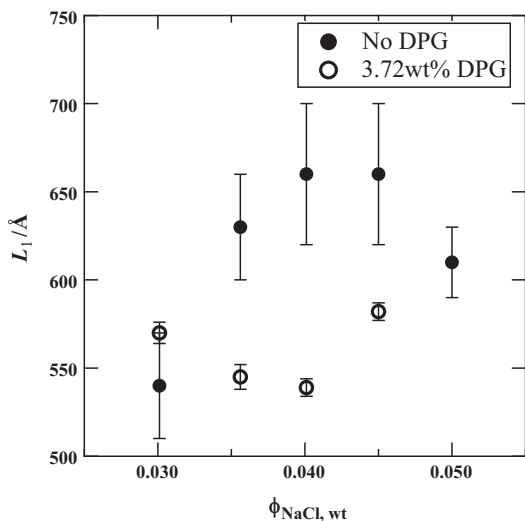


Fig. 4. Kuhn length, L_1 , versus weight fraction salt, $\phi_{\text{NaCl, wt}}$, with and without DPG showing a decrease in persistence in the presence of DPG.

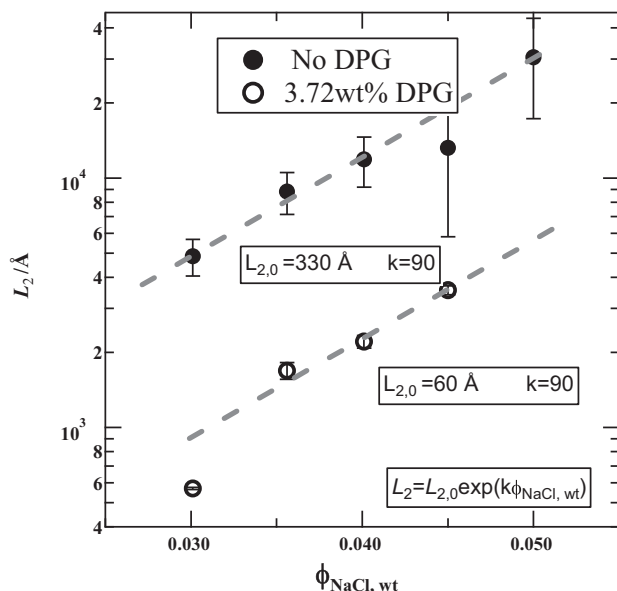


Fig. 5. L_2 versus salt concentration showing similar behavior with weight fraction salt with an exponential dependence of $L_2 = L_{2,0} \exp(k\phi_{\text{NaCl, wt}})$. $k \sim 90$ and $L_{2,0} = 60$ and 330 \AA for 0% and 3.72% DPG respectively.

$L_{2,0}$ reflects the extrapolated WLM contour length in the absence of added salt, that is just with the stoichiometric surfactant head group counter ions. In this condition, the presence of DPG has a dramatic effect on the contour length, reducing it by 80%. It can be postulated that this reduction is associated with a lower, end-cap energy relative to the energy for cylindrical segments of the WLM, i.e. reduced chain scission energy, that is associated with increased head group charge interactions with a reduced dielectric constant media as discussed above.

Despite the dramatic 80% reduction in $L_{2,0}$ with addition of DPG, the dependence on salt concentration is surprisingly identical with an exponential constant $k = 90$ irrespective of the presence of DPG. This indicates a mechanistic identity for the effect of added counter ion on micellar structure that is independent of the adjustment of the dielectric constant of the media.

According to the theory of Cates and Candau [25], the micelle contour length has an exponential dependence on the free energy

of scission. We can expect a relationship between counter ion concentration and scission energy that will be explored in future studies.

The other well-known effect of polar organic molecules is their ability to modify the organization of water molecules. Co-solvent molecules have been classified into structure breakers or makers depend on their ability of establishing H-bonds. It has been reported that the water-structuring effect of glycols is extremely weak compared with monohydric alcohols especially at low concentration [20]. It is suggested that this structure modifying ability of glycols would not have a pronounced impact on the micelle structure [31] and will therefore not be further discussed.

4.4. Specific viscosity dependence on contour length

The viscosity of WLM solutions is strongly dependent on the contour length. The specific viscosity, $\eta_{sp} = (\eta - \eta_0)/\eta_0$, is plotted against L_2 in Fig. 6, where η and η_0 are the zero-shear rate viscosity of the surfactant solution and its corresponding solvent respectively. η_{sp} shows a power-law dependence of 1 on L_2 for samples with DPG as co-solvent and samples with no co-solvent at low salt concentration; while that of samples with no co-solvent at higher salt concentration have a power law dependence of about 3/2. The power law of 1 is consistent with the typical value reported for synthetic polymer solutions with unentangled short chain polymers [34] that display Rouse behavior. In this case, the number of persistent units of the micelles varies from 1 to 5 in the presence of DPG, which is sufficiently low to display Rouse behavior [35].

A value of $\eta_{sp} = 1$, a solution viscosity about twice that of the solvent, is generally taken as indicative of the initial chain overlap [36]. The larger power-law dependence of η_{sp} on L_2 for samples with no DPG is the typical consequence of the formation of long chain micelles and micellar entanglement [37]. This seems to be the case in Fig. 5 where most of the no DPG results occur above this value. Thus, the addition of DPG has a dramatic impact on the viscoelastic properties of WLM solutions due to a dramatic reduction in L_2 associated with the lower dielectric constant media.

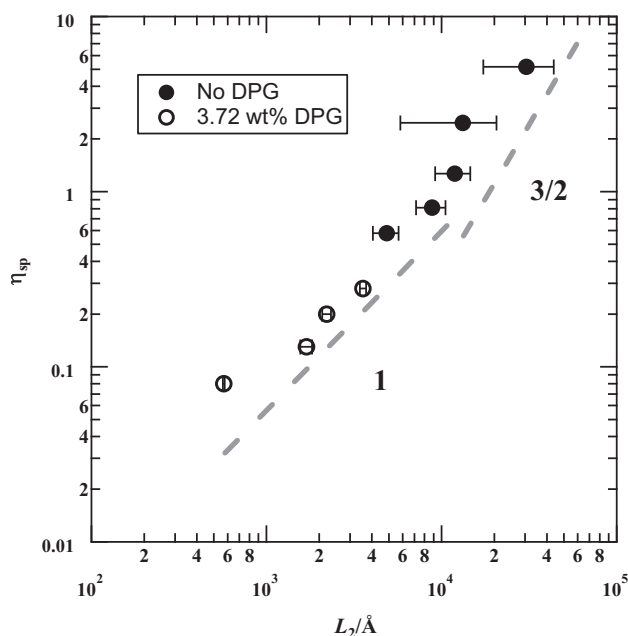


Fig. 6. Plot of η_{sp} versus L_2 showing different power law dependence for 0% and 3.72% DPG respectively.

5. Conclusion

Mixtures of SLES and CAPB have been studied in a binary solvent mixture of D₂O and DPG with addition of NaCl. The SANS data was fitted by a scattering function which allows the depiction of the hierarchical structure of WLMs [27]. Based on the measured SLD, we were able to conclude that DPG molecules mainly stay in the solvent phase for the mixed surfactant system in DPG/D₂O mixtures. The decreased dielectric constant of the solvent with addition of DPG may increase the electrostatic interaction between head groups and lead to the observed smaller micelle radii and dramatic reduction in contour length of the micelles which agrees well with most of the previous studies [8,10–17]. For the samples without DPG, an exponential increase of micelle length with increasing salt concentration is observed which is an effect commonly expected for increasing ionic strength. It is found that samples with and without DPG exhibit similar growth rate upon addition of salt. Apparently, the introduction of DPG does not interfere mechanistically with the effect of inorganic salt on micelle growth but has a dramatic impact on the extrapolated zero salt contour length by almost an order of magnitude. The influence of different co-solvents at different concentrations will be evaluated in future studies. It is also planned to investigate the impact of co-solvents on chain scission energy that is anticipated from the results of this study.

Acknowledgements

This work was funded by P&G. The work relied on the expertise and assistance of Yuri Melnichenko at GP-SANS, ORNL and Paul Butler at NG7-SANS, NIST. The National Institute of Standards and Technology, U.S. Department of Commerce provided the neutron research facilities used in this work. A portion of this research used resources at the High Flux Isotope Reactor, a DOE Office of Science User Facility operated by the Oak Ridge National Laboratory.

Appendix A. Supplementary material

Supplementary data associated with this article can be found, in the online version, at <http://dx.doi.org/10.1016/j.jcis.2017.08.090>.

References

- [1] C.A. Dreiss, Wormlike micelles: where do we stand? Recent developments, linear rheology and scattering techniques, *Soft Matter* 3 (2007) 956–970.
- [2] L.L. Schramm, *Surfactants: Fundamentals and Applications*, in: The Petroleum Industry, Cambridge University Press, Cambridge, 2000, pp. 3–22.
- [3] S. Sinha, D. Tikariha, J. Lakra, A.K. Tiwari, S.K. Saha, K.K. Ghosh, Effect of polar organic solvents on self-aggregation of some cationic monomeric and dimeric surfactants, *J. Surfactants Deterg.* 18 (2015) 629–640.
- [4] S. Kalepu, V. Nekkanti, Insoluble drug delivery strategies: review of recent advances and business prospects, *Acta Pharm. Sin.* B 5 (2015) 442–453.
- [5] C.N. Mulligan, R.N. Yong, B.F. Gibbs, Surfactant-enhanced remediation of contaminated soil: a review, *Eng. Geol.* 60 (2001) 371–380.
- [6] S. Iglauer, Y. Wu, P. Shuler, Y. Tang, W.A. Goddard, Alkyl polyglycoside surfactant–alcohol cosolvent formulations for improved oil recovery, *Colloids Surf., A* 339 (2009) 48–59.
- [7] D. Myers, *Solubilization and micellar and phase transfer catalysis*, in: *Surfactant Science and Technology*, Wiley, Hoboken, NJ, 2005, p. 191.
- [8] R. Zana, Aqueous surfactant–alcohol systems: a review, *Adv. Colloid Interface Sci.* 57 (1995) 1–64.
- [9] T.L. Brown, H.E. LeMay, B.E. Bursten, C. Murphy, P. Woodward, M.E. Stoltzfus, Properties of solutions, in: *Chemistry: the central science*, twelfth ed. Pearson Prentice Hall, Upper Saddle River, NJ, 2012, pp. 520–520.
- [10] M.S. Bakshi, Micelle formation by anionic and cationic surfactants in binary aqueous solvents, *J. Chem. Soc., Faraday Trans.* 89 (1993) 4323–4326.
- [11] C.C. Ruiz, J.A. Molina-Bolivar, J. Aguiar, G. MacIsaac, S. Moroze, R. Palepu, Thermodynamic and structural studies of Triton X-100 micelles in ethylene glycol–water mixed solvents, *Langmuir* 17 (2001) 6831–6840.
- [12] C.C. Ruiz, Thermodynamics of micellization of tetradecyltrimethylammonium bromide in ethylene glycol–water binary mixtures, *Colloid Polym. Sci.* 277 (1999) 701–707.
- [13] R. Nagarajan, C.C. Wang, Theory of surfactant aggregation in water/ethylene glycol mixed solvents, *Langmuir* 16 (2000) 5242–5251.
- [14] R. Nagarajan, C.C. Wang, Solution behavior of surfactants in ethylene glycol: probing the existence of a CMC and of micellar aggregates, *J. Colloid Interface Sci.* 178 (1996) 471–482.
- [15] K. Mukherjee, C.M. Dulal, P.M. Satya, Thermodynamics of micellization of aerosol OT in binary mixtures of water, formamide, ethylene glycol, and dioxane, *J. Phys. Chem.* 98 (1994) 4713–4718.
- [16] R. Zana, S. Yiv, C. Strazielle, P. Lianos, Effect of alcohol on the properties of micellar systems: I. Critical micellization concentration, micelle molecular weight and ionization degree, and solubility of alcohols in micellar solutions, *J. Colloid Interface Sci.* 80 (1981) 208–223.
- [17] S. Dai, K.C. Tam, Effect of cosolvents on the binding interaction between poly(ethylene oxide) and sodium dodecyl sulfate, *J. Phys. Chem. B* 110 (2006) 20794–20800.
- [18] J. Penfold, E. Staples, I. Tucker, P. Cummins, The structure of nonionic micelles in less polar solvents, *J. Colloid Interface Sci.* 185 (1997) 424–431.
- [19] P. Alexandridis, L. Yang, SANS investigation of polyether block copolymer micelle structure in mixed solvents of water and formamide, ethanol, or glycerol, *Macromolecules* 33 (2000) 5574–5587.
- [20] P.A. Kralchevsky, K.D. Danov, *Chemical Physics of Colloid Systems and Interfaces*, in: K.S. Birdi (Ed.), *Handbook of surface and colloid chemistry*, CRC Press, Boca Raton, FL, 2015, p. 276.
- [21] K.D. Danov, A.K. Peter, P.A. Kavssery, Micelle–monomer equilibria in solutions of ionic surfactants and in ionic–nonionic mixtures: a generalized phase separation model, *Adv. Colloid Interface Sci.* 206 (2014) 17–45.
- [22] I.N. Basumallick, K.K. Kundu, Thermodynamics of transfer of hydrogen halides from water to glycerol–water mixtures and the structuredness of the solvents, *Can. J. Chem.* 57 (1979) 961–967.
- [23] G. Porte, Y. Poggi, J. Appell, G. Maret, Large micelles in concentrated solutions. The second critical micellar concentration, *J. Phys. Chem.* 88 (1984) 5713–5720.
- [24] K. Vogtt, H. Jiang, G. Beaucage, M. Weaver, Free energy of scission for sodium laurth-1-sulfate wormlike micelles, *Langmuir* 33 (2017) 1872–1880.
- [25] M.E. Cates, S. Candau, Statics and dynamics of worm-like surfactant micelles, *J. Phys.: Condens. Matter.* 2 (1990) 6869–6892.
- [26] R. Ramachandran, G. Beaucage, A.S. Kulkarni, Persistence length of short-chain branched polyethylene, *Macromolecules* 41 (2008) 9802–9806.
- [27] K. Vogtt, G. Beaucage, M. Weaver, H. Jiang, Scattering function for branched wormlike chains, *Langmuir* 31 (2015) 8228–8234.
- [28] D. Firestone, *Official methods and recommended practices of the AOCS*, AOCS, Urbana, IL, 2009.
- [29] S.R. Kline, Reduction and analysis of SANS and USANS data using Igor Pro, *J. Appl. Crystallogr.* 39 (2006) 895–900.
- [30] H. Gharibi, B.M. Razavizadeh, A.A. Rafati, Electrochemical studies associated with the micellization of dodecyltrimethyl ammonium bromide (DOTAB) in aqueous solutions of ethanol and 1-propanol, *Colloids Surf., A* 136 (1998) 123–132.
- [31] G. D'Errico, D. Ciccarelli, O. Ortona, Effect of glycerol on micelle formation by ionic and nonionic surfactants at 25 °C, *J. Colloid Interface Sci.* 286 (2005) 747–754.
- [32] E. Ikada, Dielectric properties of some diols, *J. Phys. Chem.* 75 (1971) 1240–1246.
- [33] X. Tang, W. Zou, P.H. Koenig, S.D. McConaughy, M.R. Weaver, D.M. Eike, M.J. Schmidt, R.G. Larson, Multiscale modeling of the effects of salt and perfume raw materials on the rheological properties of commercial threadlike micellar solutions, *J. Phys. Chem. B* 121 (2017) 2468–2485.
- [34] G.C. Berry, T.G. Fox, The viscosity of polymers and their concentrated solutions, *Adv. Polym. Sci.* 5 (1968) 261–357.
- [35] G.R. Strobl, Microscopic dynamics, in: *The Physics of Polymers: Concepts for Understanding their Structures and Behavior*, Springer, New York, 2007, p. 317.
- [36] S. Dou, R.H. Colby, Charge density effects in salt-free polyelectrolyte solution rheology, *J. Polym. Sci. Part B Polym. Phys.* 44 (2006) 2001–2013.
- [37] T.R. Carale, D. Blanschtein, Theoretical and experimental determinations of the crossover from dilute to semi dilute regimes of micellar solutions, *J. Phys. Chem.* 96 (1992) 459–467.